

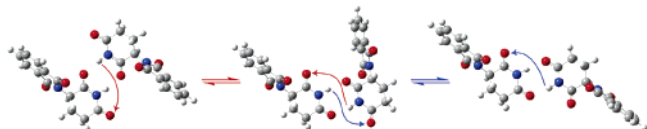
## Fliplike Motion in the Thalidomide Dimer: Conformational Analysis of (*R*)-Thalidomide Using Vibrational Circular Dichroism Spectroscopy

Hiroshi Izumi,<sup>\*,†</sup> Shigeru Futamura,<sup>†</sup> Nakako Tokita,<sup>‡</sup> and Yoshiaki Hamada<sup>‡</sup>

National Institute of Advanced Industrial Science and Technology (AIST), AIST Tsukuba West, 16-1 Onogawa, Tsukuba, Ibaraki 305-8569, Japan, and The University of the Air, 2-11 Wakaba, Mihama-ku, Chiba City, 261-8586, Japan

izumi.h@aist.go.jp

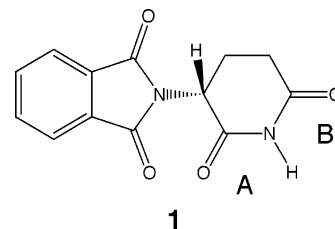
Received August 3, 2006



The dynamic fliplike motion in the (*R*)-thalidomide dimer has been reported for the first time. The vibrational circular dichroism (VCD) spectrum of (*R*)-thalidomide in DMSO-*d*<sub>6</sub> indicates the characteristic  $\nu_{\text{CO}}$  bands with opposite signs and reflects the structural property of the equatorial configuration of the phthalimide ring. On the other hand, the VCD spectrum of (*R*)-thalidomide in CDCl<sub>3</sub> exhibits a different pattern of  $\nu_{\text{CO}}$  bands and suggests the fliplike motion in dimer forms. This novel insight for the dimer forms would be helpful for the understanding of the structure–activity relationship for thalidomide.

Thalidomide is a tragic-historical compound as a human teratogen.<sup>1</sup> Recently, however, this compound has been reviewed again for its immunosuppressive, immunomodulatory, or anti-angiogenic effect on Hansen's disease, rheumatoid arthritis, Behcet's syndrome, aphthous ulcer, and multiple myeloma.<sup>2</sup> The versatile potency suggests the biological action of the simple structure of thalidomide, especially the imido part, on the important point of the human network system. The dimer form and polymorphism in the solid state have already been pointed out;<sup>3</sup> nevertheless, the contribution of the dimer structure to the

action in the solution state has not been considered.<sup>2,4</sup> The basic property of the interaction of the imido part has not been reported in detail. The antiangiogenic activity of thalidomide is a consequence of metabolic activation as demonstrated by in vivo studies.<sup>4b</sup> However, the biotransformation of thalidomide is very complex: (*R*)-thalidomide is preferentially metabolized in the 2',6'-dioxopiperidine-3'-yl moiety, whereas (*S*)-thalidomide is mainly transformed by hydroxylation in the phthalimide ring. Further, (3'*R*,5'*R*)-*trans*-5'-hydroxythalidomide epimerizes to the thermodynamically more stable (3'*S*,5'*R*)-*cis*-isomer.<sup>4a</sup> At present, the identity of the active species has not been confirmed.<sup>4b</sup>



Vibrational circular dichroism (VCD) spectroscopy<sup>5</sup> is highly sensitive to the conformations of chiral molecules. Recently, we have shown that the well-known odd–even effect of chiral alcohols in the solution state can be theoretically interpreted using VCD in terms of their conformations and associated vibrational mode patterns.<sup>6</sup> VCD spectroscopy is also effective in analyzing highly assembled forms of supramolecular species.<sup>7</sup> Here, we show the VCD spectra of (*R*)-thalidomide (**1**) and demonstrate theoretically the dynamic fliplike motion of the (*R*)-thalidomide dimer (**2**) in CDCl<sub>3</sub> for the first time.

Figure 1a shows the VCD and IR spectra of **1** (DMSO-*d*<sub>6</sub>, 0.50 M, CaF<sub>2</sub>, 5  $\mu\text{m}$  path length). The characteristic  $\nu_{\text{CO}}$  VCD bands with opposite signs (1721 cm<sup>-1</sup>,  $\Delta\epsilon = 1.6 \times 10^{-1}$ ; 1709 cm<sup>-1</sup>,  $\Delta\epsilon = -1.7 \times 10^{-1}$ ) were observed. To assign these bands, the conformational and vibrational analyses of monomer

(4) (a) Meyring, M.; Mühlbacher, J.; Messer, K.; Kastner-Pustet, N.; Bringmann, G.; Mannschreck, A.; Blaschke, G. *Anal. Chem.* **2002**, *74*, 3726–3735. (b) Luzzio, F. A.; Duveau, D. Y.; Lepper, E. R.; Figg, W. D. *J. Org. Chem.* **2005**, *70*, 10117–10120. (c) Noguchi, T.; Fujimoto, H.; Sano, H.; Miyajima, A.; Miyachi, H.; Hashimoto, Y. *Bioorg. Med. Chem. Lett.* **2005**, *15*, 5509–5513.

(5) (a) Cheeseman, J. R.; Frisch, M. J.; Devlin, F. J.; Stephens, P. J. *Chem. Phys. Lett.* **1996**, *252*, 211–220. (b) Nafie, L. A.; Dukor, R. K.; Freedman, T. B. In *Handbook of Vibrational Spectroscopy*; Chalmers, J. M., Griffiths, P. R., Eds.; John Wiley & Sons, Ltd.: Chichester, 2002; pp 731–744. (c) Wang, F.; Wang, Y.; Polavarapu, P. L.; Li, T.; Drabowicz, J.; Pietrusiewicz, K. M.; Zygo, K. *J. Org. Chem.* **2002**, *67*, 6539–6541. (d) Freedman, T. B.; Cao, X. L.; Dukor, R. K.; Nafie, L. A. *Chirality* **2003**, *15*, 743–758. (e) Izumi, H.; Futamura, S.; Nafie, L. A.; Dukor, R. K. *Chem. Rec.* **2003**, *3*, 112–119. (f) Furo, T.; Mori, T.; Wada, T.; Inoue, Y. *J. Am. Chem. Soc.* **2005**, *127*, 8242–8243. (g) Vargas, A.; Bonalumi, N.; Ferri, D.; Baiker, A. *J. Phys. Chem. A* **2006**, *110*, 1118–1127. (h) Brotin, T.; Cavagnat, D.; Dutasta, J.-P.; Buffeteau, T. *J. Am. Chem. Soc.* **2006**, *128*, 5533–5540. (i) Monde, K.; Miura, N.; Hashimoto, M.; Taniguchi, T.; Inabe, T. *J. Am. Chem. Soc.* **2006**, *128*, 6000–6001. (j) Naubron, J.-V.; Giordano, L.; Fotiadu, F.; Bürgi, T.; Vanthuyne, N.; Roussel, C.; Buono, G. *J. Org. Chem.* **2006**, *71*, 5586–5593. (k) Kuppens, T.; Herrebout, W.; van der Veken, B.; Bultinck, P. *J. Phys. Chem. A* **2006**, *110*, 10191–10200. (l) Gautier, C.; Bürgi, T. *J. Am. Chem. Soc.* **2006**, *128*, 11079–11087.

(6) Izumi, H.; Yamagami, S.; Futamura, S.; Nafie, L. A.; Dukor, R. K. *J. Am. Chem. Soc.* **2004**, *126*, 194–198.

(7) Urbanová, M.; Setnička, V.; Devlin, F. J.; Stephens, P. J. *J. Am. Chem. Soc.* **2005**, *127*, 6700–6711.

<sup>†</sup> National Institute of Advanced Industrial Science and Technology.

<sup>‡</sup> The University of the Air.

(1) (a) Lenz, W. *Dtsch. Med. Wochenschr.* **1961**, *86*, 2555–2556. (b) McBride, W. G. *Lancet* **1961**, *278*, 1358.

(2) (a) Calabrese, L.; Fleischer, A. B. *Am. J. Med.* **2000**, *108*, 487–495. (b) Li, P. K.; Pandit, B.; Sackett, D. L.; Hu, Z. G.; Zink, J.; Zhi, J. D.; Freeman, D.; Robey, R. W.; Werbovetz, K.; Lewis, A.; Li, C. L. *Mol. Cancer Ther.* **2006**, *5*, 450–456. (c) Deng, L.; Ding, W. H.; Granstein, R. D. *J. Invest. Dermatol.* **2003**, *121*, 1060–1065. (d) Arbiser, J. L.; Johnson, D.; Cohen, C.; Brown, L. F. *J. Cutan. Med. Surg.* **2003**, *7*, 225–228. (e) Thomas, D. A.; Giles, F. J.; Albitar, M.; Cortes, J. E.; Verstovsek, S.; Faderl, S.; O'Brien, S. M.; Garcia-Manero, G.; Keating, M. J.; Pierce, S.; Zeldis, J.; Kantarjian, H. M. *Cancer* **2006**, *106*, 1974–1984.

(3) Reepmeyer, J. C.; Rhodes, M. O.; Cox, D. C.; Silvertown, J. V. *J. Chem. Soc., Perkin Trans.* **1994**, *2*, 2063–2067.

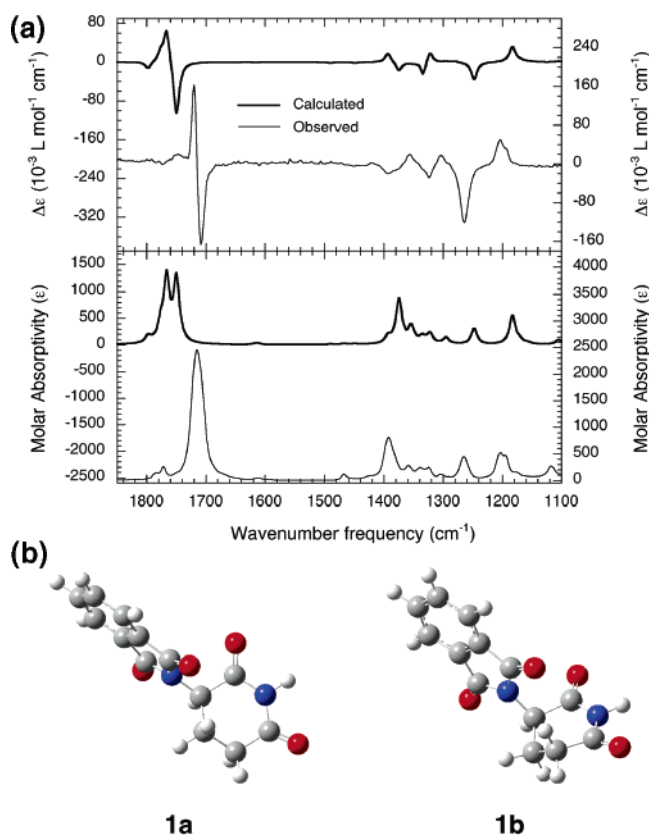


**FIGURE 1.** (a) Comparison of the measured VCD ( $\Delta\epsilon$ ) and IR ( $\epsilon$ ) spectra of **1** (DMSO- $d_6$ , 0.50 M, CaF<sub>2</sub>, 5  $\mu\text{m}$  path length) with the predicted spectra for **1a** (B3LYP/6-31G\*). (b) Optimized geometry of conformers **1a** and **1b** (B3LYP/6-31G\*).

**1** were carried out using density functional theory calculations.<sup>8</sup> Two major conformers, **1a** and **1b**, were optimized (Figure 1b). The difference between the two conformers was the configuration (axial or equatorial) of the phthalimide rings. Conformer **1a** is more stable than **1b** due to the diminished steric repulsion ( $\Delta G = 2.16$  kcal/mol). The measured VCD spectrum of **1** is in good agreement with the predicted VCD spectrum for **1a** (Figure 1a). The VCD spectrum of **1** strongly reflects the structural property of the equatorial configuration of the phthalimide ring.<sup>9</sup>

On the other hand, the different pattern of  $\nu_{\text{CO}}$  bands for the VCD spectrum of **1** (0.005 M, BaF<sub>2</sub>, 489  $\mu\text{m}$  path length) in CDCl<sub>3</sub> was observed (1748  $\text{cm}^{-1}$ ,  $\Delta\epsilon = 5.8 \times 10^{-2}$ ; 1728  $\text{cm}^{-1}$ ,  $\Delta\epsilon = 1.4 \times 10^{-1}$ ; 1719  $\text{cm}^{-1}$ ,  $\Delta\epsilon = -1.6 \times 10^{-1}$ ) (Figure 2a).

(8) Frisch, M. J.; Trucks, G. W.; Schlegel, H. B.; Scuseria, G. E.; Robb, M. A.; Cheeseman, J. R.; Montgomery, J. A., Jr.; Vreven, T.; Kudin, K. N.; Burant, J. C.; Millam, J. M.; Iyengar, S. S.; Tomasi, J.; Barone, V.; Mennucci, B.; Cossi, M.; Scalmani, G.; Rega, N.; Petersson, G. A.; Nakatsuji, H.; Hada, M.; Ehara, M.; Toyota, K.; Fukuda, R.; Hasegawa, J.; Ishida, M.; Nakajima, T.; Honda, Y.; Kitao, O.; Nakai, H.; Klene, M.; Li, X.; Knox, J. E.; Hratchian, H. P.; Cross, J. B.; Bakken, V.; Adamo, C.; Jaramillo, J.; Gomperts, R.; Stratmann, R. E.; Yazyev, O.; Austin, A. J.; Cammi, R.; Pomelli, C.; Ochterski, J. W.; Ayala, P. Y.; Morokuma, K.; Voth, G. A.; Salvador, P.; Dannenberg, J. J.; Zakrzewski, V. G.; Dapprich, S.; Daniels, A. D.; Strain, M. C.; Farkas, O.; Malick, D. K.; Rabuck, A. D.; Raghavachari, K.; Foresman, J. B.; Ortiz, J. V.; Cui, Q.; Baboul, A. G.; Clifford, S.; Cioslowski, J.; Stefanov, B. B.; Liu, G.; Liashenko, A.; Piskorz, P.; Komaromi, I.; Martin, R. L.; Fox, D. J.; Keith, T.; Al-Laham, M. A.; Peng, C. Y.; Nanayakkara, A.; Challacombe, M.; Gill, P. M. W.; Johnson, B.; Chen, W.; Wong, M. W.; Gonzalez, C.; Pople, J. A. *Gaussian 03*, revision C.02; Gaussian, Inc.: Wallingford, CT, 2004.

(9) See Supporting Information.

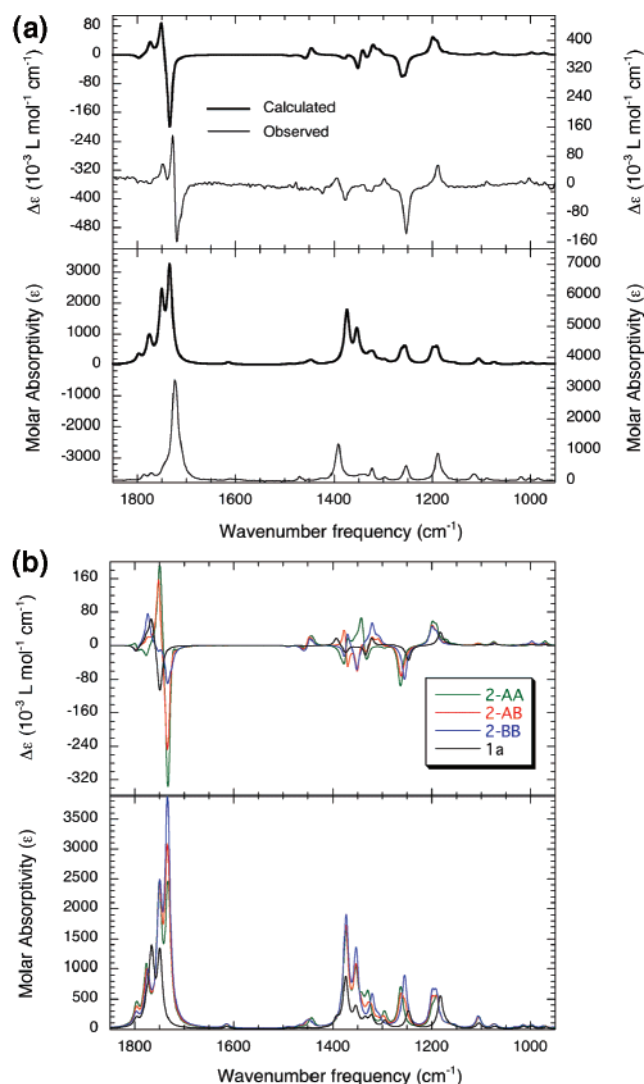


**FIGURE 2.** (a) Comparison of the measured VCD ( $\Delta\epsilon$ ) and IR ( $\epsilon$ ) spectra of **1** (CDCl<sub>3</sub>, 0.005 M, BaF<sub>2</sub>, 489  $\mu\text{m}$  path length) with the predicted (population weighted) spectra for **1a** (B3LYP/6-31G\*). (b) Predicted VCD ( $\Delta\epsilon$ ) and IR ( $\epsilon$ ) spectra of **2-AA**, **2-AB**, **2-BB**, and **1a** (B3LYP/6-31G\*).

The VCD spectra of **1** in CD<sub>2</sub>Cl<sub>2</sub> and CD<sub>3</sub>CN also indicate a similar pattern of  $\nu_{\text{CO}}$  bands. The  $\nu_{\text{CO}}$  VCD bands for a higher concentration of **1** (0.04 M) were slightly broadened but not essentially changed.<sup>9</sup> The two  $\nu_{\text{CO}}$  positive VCD bands and the  $\nu_{\text{NH}}$  IR band at 3366  $\text{cm}^{-1}$  strongly suggest the existence of the (*R*)-thalidomide dimer (**2**).<sup>9</sup> (*R*)-Thalidomides **1** can be connected with each other through the imido parts **A** or **B**. The density functional theory calculations indicate the existence of three conformational isomers of **2**, **2-AA**, **2-AB**, and **2-BB** (Figure 3). The predicted (population weighted) VCD bands of **2** (three conformers) correspond well to those observed in CDCl<sub>3</sub> solution (Figure 2a). The  $\nu_{\text{CO}}$  band at 1748  $\text{cm}^{-1}$  is assigned as the contribution of conformer **2-BB**, but in contrast, the  $\nu_{\text{CO}}$  band at 1728  $\text{cm}^{-1}$  is assigned as the contribution of conformers **2-AA** and **2-AB** (Figure 2b). The observed VCD spectrum of **1** suggests the fliplike motion of dimer forms **2** in CDCl<sub>3</sub>. Recently, Vass and co-workers have reported that  $\beta$ -lactams also tend to form H-bonded dimers in CDCl<sub>3</sub>, but the population

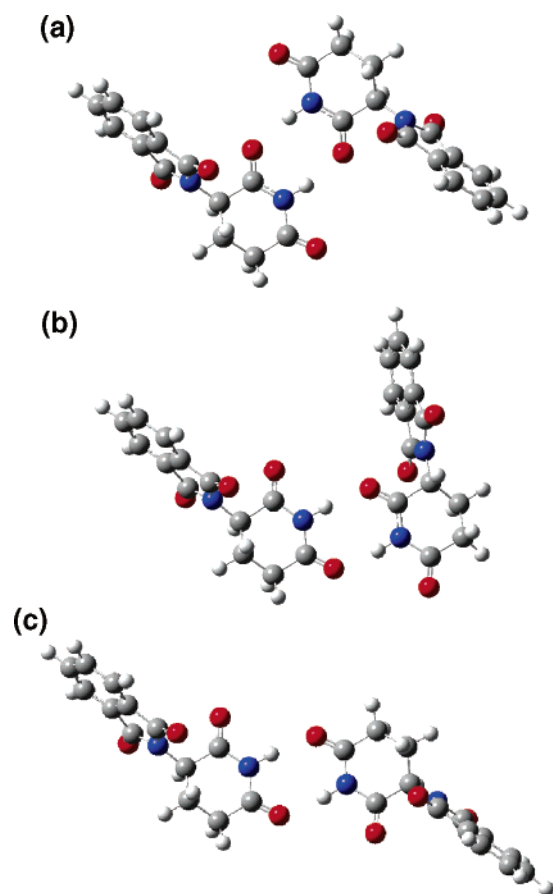


**FIGURE 3.** (a) Optimized geometry of conformer **2-AA** (B3LYP/6-31G\*). (b) Optimized geometry of conformer **2-AB** (B3LYP/6-31G\*). (c) Optimized geometry of conformer **2-BB** (B3LYP/6-31G\*).

of H-bonded dimers is small.<sup>10</sup> In the case of thalidomide, only one observed  $\nu_{\text{NH}}$  IR band suggests that the contribution of the entirely free monomer is small. The planarity of the CONHCO moiety is high, and the inversion around the N atom is suppressed. The predicted (population weighted) IR bands of **2** (three conformers) are slightly different from the observed IR ones (Figure 2a). This suggests the contribution of the H-bonded species among conformers **2-AA**, **2-AB**, and **2-BB**. The  $\nu_{\text{NH}}$

(10) Vass, E.; Hollósi, M.; Forró, E.; Fülöp, F. *Chirality* **2006**, *18*, 733–740.

IR band was slightly shifted in higher concentration (0.046 M, 3368  $\text{cm}^{-1}$ ). The increased force constant of the N–H bond for **2** suggests the further intermolecular interaction such as that seen in the crystal structure.<sup>3</sup>

From these results, we revealed the dynamic intermolecular interaction of the imido part for (*R*)-thalidomide **1**. This novel insight for the dimer forms **2** would be helpful for the understanding of the structure–activity relationship for thalidomide. VCD spectroscopy would be available as a powerful complement to NMR spectroscopy that leads to significantly improved SAR studies. Further conformational analysis of (*R*)-thalidomide **1** in DMSO-*d*<sub>6</sub> is now in progress.

### Experimental Section

**Measurements.** All reagents were of commercial grade. The VCD spectra of the solution state were recorded with 3–5 h data collection time at 4  $\text{cm}^{-1}$  resolution. The DMSO-*d*<sub>6</sub> solutions were placed in a 5  $\mu\text{m}$  path length cell with CaF<sub>2</sub> windows. The CDCl<sub>3</sub>, CD<sub>2</sub>Cl<sub>2</sub>, and CD<sub>3</sub>CN solutions were placed in a 72 or 489  $\mu\text{m}$  path length cell with BaF<sub>2</sub> windows. The VCD baseline was obtained from the average spectrum of *R*- and *S*-enantiomers.

**Calculations.** All geometry optimizations, conformer searches, vibrational frequencies, and absorption and VCD intensities for **1** and **2** were calculated using the Gaussian 03 program<sup>8</sup> on a Pentium 4 (3.2 GHz) PC. Density functional theory with B3LYP functional and 6-31G(d) basis sets was used for the calculations. The theoretical absorption and VCD spectra were simulated with Lorentzian band shapes and 6  $\text{cm}^{-1}$  full width at half-height. The ab initio frequencies were scaled by 0.97, and the thermal corrections to Gibbs free energies were scaled with 0.9989.

**Acknowledgment.** This work was partly supported by the Industrial Technology Research Grant Program from the New Energy and Industrial Technology Development Organization of Japan. We thank Prof. L. A. Nafie and Dr. R. K. Dukor for fruitful discussions.

**Supporting Information Available:** Relative Gibbs free energies and populations of conformations **1** and **2**; anisotropy ratio of  $\nu_{\text{CO}}$  bands; Cartesian coordinates of conformations **1** and **2**; observed and calculated VCD spectra of **1** with IR spectra in DMSO-*d*<sub>6</sub> and CDCl<sub>3</sub>; and observed and calculated anisotropy ratios of **1** in DMSO-*d*<sub>6</sub> and CDCl<sub>3</sub>. This material is available free of charge via the Internet at <http://pubs.acs.org>.

JO061612Q